A comparative simulation study of coupled THM processes and their effect on fractured rock permeability around nuclear waste repositories

Jonny Rutqvist[1*], Deborah Barr[2], Jens T. Birkholzer[1], Kiyoshi Fujisaki[3], Olaf Kolditz[4], Quan-Sheng Liu[5], Tomoo Fujita[3] Wenqing Wang[4], Cheng-Yuan Zhang[5]

[1] Earth Sciences Division, Lawrence Berkeley National Laboratory, MS 90-1116, Berkeley, CA 947 20, USA

[2]Office of Repository Development, U.S. Department of Energy, Las Vegas, USA

[3]Japan Atomic Energy Agency, Tokai, Japan

[4]Helmholtz Center for Environmental Research, Leipzig, Germany

[5]Chinese Academy of Sciences, Wuhan, China

* Corresponding author. Tel.: +1-510-486-5432, fax.: +1-510-486-5432
E-mail address: Jrutqvist@lbl.gov (J. Rutqvist)

Prepared for publication in Environmental Geology

DECOVALEX-THMC Special Issue

Abstract

This paper presents an international, multiple-code, simulation study of coupled thermal, hydrological, and mechanical (THM) processes and their effect on permeability and fluid flow in fractured rock around heated underground nuclear waste emplacement drifts. Simulations were conducted considering two types of repository settings: (a) open emplacement drifts in relatively shallow unsaturated volcanic rock, and (b) backfilled emplacement drifts in deeper saturated crystalline rock. The results showed that for the two assumed repository settings, the dominant mechanism of changes in rock permeability was thermal-mechanically-induced closure (reduced aperture) of vertical fractures, caused by thermal stress resulting from repository-wide heating of the rock mass. The magnitude of thermal-mechanically-induced changes in permeability was more substantial in the case of an emplacement drift located in a relatively shallow, low-stress environment where the rock is more compliant, allowing more substantial fracture closure during thermal stressing. However, in both of the assumed repository settings in this study, the thermal-mechanically induced changes in permeability caused relatively small changes in the flow field, with most changes occurring in the vicinity of the emplacement drifts.

Keywords:

coupled processes, nuclear waste repository, temperature, stress, permeability.

1 Introduction

This paper presents results from an international, multiple-team simulation study of coupled thermal, hydrological, and mechanical (THM) interactions and their impact on permeability and fluid flow around heated underground nuclear waste emplacement drifts in fractured rock. The study was part of the DECOVALEX-THMC project (2004 through 2007), which was the fourth in a series of DECOVALEX

(an acronym for DEvelopment of COupled models and their VALidation against EXperiments) projects that were first established in 1992 by a number of national regulatory authorities and nuclear waste management organizations (Tsang et al. 2008). The added "C" in DECOVALEX-THMC stands for chemical processes. However, the study presented in this paper is focused on THM processes and their impact on fractured rock permeability and fluid flow. This includes heating of the rock mass by the waste package and the resulting thermal-mechanically induced changes in rock stress and fractured rock permeability, as well as their impact on the flow field around emplacement drifts. These changes in rock permeability may be more important for repository performance if they are permanent (irreversible), in which case they would persist after the thermal conditions have returned to ambient—that is, they would affect the entire compliance period.

Two generic repository types with horizontal emplacement tunnels are considered in this study:

Type A—A high-temperature (above boiling) repository in a deep, unsaturated volcanic rock formation, with emplacement in open gas-filled tunnels, similar to the Yucca Mountain repository concept in the United States.

Type B—A low-temperature (below boiling) repository in a deep saturated crystalline rock formation, with emplacement in back-filled tunnels, a concept considered in a number of European countries.

The initial rock properties for the two repository types were derived from characterization of two major *in situ* experimental sites that have been part of previous DECOVALEX project phases. The first one, representing Repository Type A, is the Yucca Mountain Drift Scale Test, conducted at Yucca Mountain,

Nevada (Rutqvist et al. 2005a). The second one, representing Repository Type B, is the FEBEX *in situ* experiment, conducted at the Grimsel Test Site, Switzerland (Alonso et al. 2005). THM simulations of these two major field experiments under a previous DECOVALEX project have already demonstrated that the short-term (i.e. occurring over several years) coupled THM processes are well understood. In the present study, however, the models are extended and used to predict coupled THM processes for the two repository types over tens of thousands of years.

Four international teams from China, Germany, Japan, and USA participated in this study, using five different numerical simulators for coupled THM analysis (see Table 1). Among the five simulators, two main approaches can be distinguished. Three simulators—ROCMAS, THAMES, and FRT-THM—are based on a single-phase fluid flow approach, whereas two simulators—TOUGH-FLAC and Geosys/Rockflow—are based on a two-phase fluid flow (liquid and gas) approach. Several of these simulators have been applied in previous DECOVALEX projects for simulation of coupled processes in systems similar to either one or the other of the repository settings (see Table 1 for a short description of each numerical simulator with source references). In this research task, the codes were adapted and used to simulate coupled THM processes for both of the two repository types.

The simulation study consisted of two distinct parts. First, an initial model inception was conducted to calculate the basic THM responses and stress evolution without considering mechanically induced changes in rock properties. The purpose of the model inception was for the research teams to familiarize themselves with the problem by performing one simulation in which all the properties were explicitly provided. In the second phase, the research teams were to develop their model and input material properties from available site data, with the ultimate goal of predicting mechanically induced changes in

hydrological properties and their impact on the flow field. Results of the model inception phase and detailed comparison of the basic THM responses are presented in Rutqvist et al. (2008a). A detailed description of this task within the DECOVALEX-THMC project and a complete set of results are reported in Birkholzer et al. (2008). This paper is focused on the second phase, i.e. prediction of mechanically induced changes in hydrological properties and their impact on the flow field for the two repository types over tens of thousands of years. It provides a unique multi-team model comparison of the coupled THM behavior around emplacement drifts of two widely different repository concepts leading to more general conclusions on the impact of mechanically induced changes in fractured rock permeability on repository performance.

This paper first briefly presents the model setup and summarizes the main coupled THM responses from the model inception phase. It is shown that the basic THM responses are well understood and that the regional thermal-mechanically-induced stresses can be calculated with confidence. Thereafter, the evolution of the stress field is studied to determine potential mechanisms of mechanically induced changes in permeability. It is shown that for the repository settings considered, the potential for shear-enhanced-permeability is small, whereas the dominant mechanisms for changes in permeability are regional thermal stressing and closure of vertical fractures (to a smaller aperture). Finally, the permeability changes and associated impact on fluid flow around the repository drifts are evaluated. Throughout the paper, a side-by-side comparison of the results for the two repository settings is conducted, which shows that the dominant mechanism for changing permeability is the same, but that differences in the repository settings (such as depths and initial stress) have an impact on the estimated magnitude of permeability changes.

2 Model Setup

The simulations were conducted using two-dimensional drift-scale models containing one horizontal emplacement drift, which had different dimensions and thermal load for each repository type (Fig. 1, Table 2). As shown in Fig. 1, because of repetitive lateral symmetry, the models extend horizontally to the mid-distance between two drifts. The lateral boundaries (vertical sides of the model) permit no flow of fluid or heat across the boundaries and a zero-displacement restriction is applied for the displacement normal to the boundary surfaces. The top boundary, representing the ground surface, was free to move, but with a fixed temperature and pressure, whereas the bottom boundary had a zero-displacement restriction for displacement normal to the boundary at a fixed temperature and pressure.

The initial conditions for the two types were different, corresponding to the respective repository settings (Table 3). Repository Type A is located at a depth of 250 m with a relatively low initial horizontal stress and high vertical stress (the maximum principal stress). The rock is highly fractured and partially saturated, with most of the liquid water sucked into the rock matrix, whereas the well-connected fracture system is almost completely dry at initial (ambient temperature) conditions. The groundwater table is located at the bottom of the model (550 m depth), and gravity-driven vertical flow is controlled by an infiltration rate of 6 mm/year at the top of the model. Repository Type B is located at depth of 500 m in denser rock, and consequently in situ stresses are much higher, especially the maximum horizontal stress. The rock is initially fully saturated with the groundwater table located at the top of the model. A vertical gradient in the hydraulic head is assumed by assigning a constant pressure slightly less than hydrostatic at the bottom boundary. This results in a slight vertical flow of 0.3 mm/year, which was used for studying the impact of permeability changes on groundwater flow around the emplacement drift. Although a near vertical flow gradient is not unrealistic if the repository is located below a recharge area, the vertical flow

gradient for the Type B repository was imposed merely for comparison of relative change in vertical fluid flow.

Table 4 presents some of the basic THM properties defined for the model inception phase. For the model inception phase, all the teams used exactly the same input properties, no data or model uncertainties were considered, and intrinsic hydrologic properties were assumed to be constant, i.e., not impacted by changes in stress. In the second phase, the research teams used the same basic material properties, but derived additional properties for analyzing mechanically induced changes in hydrologic properties. The most relevant for this study is the derivation of a relationship between thermally induced stress and rock mass permeability, which is described in Section 5.1 below.

3 Results of Basic THM Responses and Stress Evolution

Figure 2 schematically summarizes the simulation results of basic coupled THM responses and stress evolution. A regional temperature increase, ΔT, is the main driving force changing the stress field at the regional scale as well as near the drift. The thermal stress increases substantially in the horizontal direction, because the rock mass is laterally confined (Fig. 2a). The vertical stress, on the other hand, is much less affected, because the free-moving ground surface allows for vertical expansion of the rock mass. The regional thermal stressing in the horizontal direction is amplified at the drift wall by stress redistribution, causing compressive stress concentrations at the top and bottom of the drift and stress relief at the right and left sides (Fig. 2c). The thermal stress peaks around 100 to 1,000 years after emplacement, as a result of the peaking regional temperature field. The thermal stress vanishes as the temperature returns to ambient after about 10,000 to 100,000 years (Fig. 2b).

In addition to thermal-mechanical responses, complex thermal-hydrological interactions occur in the near field for both Repository Types A and B (Fig. 2c). In the case of Type A, high temperatures cause boiling and complex heat-pipe effects, which result in drying of the rock near the drift wall. The simulation results indicate that such a dryout zone exists as long as the rock temperature near the drift exceeds the boiling point, which it does for a time period between 50 to about 1,000 years. In the case of Type B, thermal-hydrological interactions are most prominent within the bentonite buffer associated with resaturation of an initially partially saturated bentonite (Rutqvist et al. 2008a).

Figures 3 and 4 show comparisons of temperature and stress evolutions from five different model simulations. Generally good agreements were achieved for both temperature and stress evolution, especially in the case of Type A (Fig. 3a and 4a). The more significant deviations in temperature evolution for Point V1 of Type B (Fig. 3b) can be explained by differences in the use of saturation-dependent thermal conductivity in the backfill (Rutqvist et al. 2008a). Some of the deviations in stress at Point V3 at the drift wall can be attributed to discretization differences (related to element size and the exact location of Point V3 in the numerical grid of the respective model). At Points V6 and H6, located away from the drift, the agreement between the results of all research teams is very good (Figs. 3 and 4). The near-field thermal-hydrological processes have a negligible effect on the regional temperature field, which implies that the basic thermal-mechanical stresses can be predicted using relatively simple models, without the need for detailed simulations of complex near-field thermal-hydrological processes (Rutqvist et al. 2008a).

Figure 5 presents the regional evolution of the stress field, using the same scales on the stress axis to emphasize the main differences in thermal-mechanical responses in Types A and B. The differences can

be related to the evolution of the heat-power and the thermal stress in comparison with the initial stress field. In Type A, the thermally induced stresses are a little lower, but at the same time, the initial stresses in that case are much smaller. Furthermore, in Type A, the thermal stresses cause the principal stresses to rotate from the initial maximum principal stress being vertical to becoming horizontal at the time of peak thermal stress. In Type B, on the other hand, the stresses are initially already relatively high, with the maximum principal stress being horizontal. In this case, the thermal stressing provides an additional increase in the horizontal stress, without a rotation of the principal stress field.

4 Potential for Fracture-Shear-Enhanced Permeability

The potential for permeability changes induced by shear slip along pre-existing fractures (shear stress reactivation) was evaluated by the DOE team, through studying the evolution of the principal stresses and comparing them to a Coulomb shear-failure criterion. For example, a Coulomb coefficient of friction μ = 0.6 is the lower-limit value observed for hydraulic conducting fractures and their correlation with maximum shear stress in fractured rock masses (e.g., Barton et al. 1995). This finding indicates that over the long term, a shear over effective normal stress ratio (τ/σ'_n) exceeding 0.6 on a fracture can lead to enhanced permeability. Considering the conservative (bounding) case that a fracture could exist at any point with an arbitrary orientation, the $\tau/\sigma'_n = 0.6$ would correspond to a principal effective stress ratio of ($\sigma'_1/\sigma'_3 = 3.12$). The factor 3.12 can be derived by reformulating the Coulomb criterion from τ/σ'_n-space to σ'_1/σ'_3-space (see Jaeger and Cook, 1979). Thus, if σ'_1 is about 3 times σ'_3, then shear-enhanced permeability could occur.

Fig. 6 presents the paths of the principal stresses at a point representing the conditions at the repository elevation but away from the emplacement drift. Included in the figure are also lines representing the principal stress ratios that could be sustained for different coefficients of friction for pre-existing fractures. For both repository types, the principal stress path shows a loop-like behavior, but in the case of elastic rock mass behavior, the principal stress state returns to its initial state when the temperature has returned to ambient conditions after more than 10,000 years.

For Type A, the initial stress field is quite low at a stress ratio corresponding to $\mu = 0.4$ (Fig. 6a). The thermal stressing causes the principal stresses to rotate, from the initial maximum principal stress being vertical to becoming horizontal at the time of peak thermal stress. A maximum stress ratio corresponding to $\mu = 0.5$ is achieved from about 100 to 1,000 years. Thereafter, the thermal stresses and the stress ratio start to decrease. Overall, the stress ratio for Type A is less than 0.6, meaning that a shear-induced permeability increase is unlikely away from the drift.

For Type B, the initial stress ratio corresponds to $\tau/\sigma'_n = 0.7$ (Fig. 6b). Such a high stress ratio (above 0.6) indicates that some fractures may already be critically stressed, i.e., on the verge of shear failure or actively slipping. During the first 10 years, the principal stress field moves away from failure, with a stress ratio declining to 0.6. However, from about 100 to 1,000 years, the stress state then moves toward a higher stress ratio and achieves a stress ratio corresponding to $\tau/\sigma'_n = 0.8$ or higher. Because σ'_1 is horizontal and σ'_3 vertical throughout the 100,000 years period, shear slip would preferentially occur in shallowly dipping fractures (dipping, about 30°). Steeply dipping fractures could not slip, because high horizontal stress would tend to compress those fractures, increasing their shear resistance.

In summary, the results of the analysis indicate that shear-induced permeability changes are unlikely, especially for the stress conditions at Repository Type A. For Repository Type B, shallowly dipping fractures may already be critically stressed and may slip further during the heating period. However, according to the site description of Type B, shallowly dipping fractures are minor cooling joints of limited extent (Birkholzer et al. 2008). Therefore, widespread shear-enhanced permeability would be unlikely for both repository settings.

5 Estimate of Permeability Change by Fracture Normal Stress

Considering that shear-induced permeability change would be unlikely, all the research teams focused on estimating potential changes in permeability as a result of changes in normal stress across vertical fractures (normal stress reactivation). Each team developed stress-versus-permeability relationships that were then used to estimate the evolution of the permeability. In this section, we compare each team's estimated stress-versus-permeability function and the calculated permeability evolution for the two repository settings.

5.1 Stress- versus-Permeability Functions

Figure 7 presents the estimated stress-versus-permeability functions derived by each research team. These functions were derived by (1) adopting a nonlinear relationship between fracture permeability and normal stress, (2) adopting a conceptual geometric model of the fractured media, and (3) calibrating required input parameters against data on stress-induced changes in fracture permeability. From the descriptions of both Type A and Type B repository settings, the fracture system could be approximated by three

orthogonal sets, one of which is horizontal and two of which are vertical (Birkholzer et al. 2008). It was recognized that the calibration should (if at all possible) be conducted against site-specific field data, rather than small scale laboratory samples, because of issues related to sampling difficulties and scale dependencies of stress-versus-flow properties of rock fractures (Rutqvist and Stephansson 2003).

In the Type A setting, the stress-versus-permeability functions were derived from observations at several field experiments that have been conducted in welded and fracture tuff at Yucca Mountain. These include the G-tunnel heated block experiments (Zimmerman et al. 1985; Zimmerman et al. 1986), the Single Heater Test (Tsang and Birkholzer 1999), niche excavation experiments (Wang and Cook 2005; Rutqvist and Stephansson 2003), and the Yucca Mountain Drift Scale Test (Rutqvist et al. 2005; Rutqvist et al. 2008b). Based on these field observations, the stress-versus-permeability functions were calibrated to achieve upon excavation a maximum of 1 to 2 orders-of-magnitude change in permeability close to the drift wall, as well as a permeability reduction limited to 1 to 2 orders of magnitude upon heating. Moreover, based on observations at the Yucca Mountain drift scale test, it was concluded that while shear slip along pre-existing fractures may induce local permeability increases, widespread increases of permeability in the rock mass (by orders of magnitude) would be unrealistic (Birkholzer et al. 2008).

For Type A, three out of four research teams (DOE, JAEA, BGR) derived their stress-versus-permeability function using the following exponential stress-versus-aperture function:

$$b = b_r + b_m = b_r + b_{\max}\left[\exp\left(\alpha\sigma'_n\right)\right] \tag{1}$$

where b_r is a residual aperture, b_m is a mechanical aperture, b_{max} is the mechanical aperture corresponding to zero normal stress, and α is a parameter related to the curvature of the function (Rutqvist et al. 2005a). The rock-mass permeability was then derived using the cubic law and a fractured model containing three

orthogonal fracture sets. The CAS team, on the other hand, used an exponential function that relates permeability to stress changes directly, without going through aperture change and cubic law (Birkholzer et al. 2008).

For the Type A setting, the resulting stress-versus-permeability functions derived by each team were different, depending on assumptions made during the calibration against the Yucca Mountain field data (Fig. 7a). The DOE team derived two alternative models (DOE1 and DOE2) that were quite different, because different conceptual models were assumed for each model when interpreting some of the permeability measurements performed at the Yucca Mountain Drift Scale Test. When deriving the DOE1 function, it was assumed that permeability changes measured at the Yucca Mountain Drift Scale Test were the result of aperture changes in the three orthogonal fracture sets (Rutqvist et al. 2005). When deriving the DOE2 function, on the other hand, it was assumed that measured permeability changes were determined by aperture changes in one dominant fracture set, which was oriented normal to the axis of the measurement boreholes (Rutqvist et al. 2008b). JAEA used Equation (1) and a conceptual model of three orthogonal fractures sets, and therefore found a stress-versus-permeability function very similar to that of DOE1. CAS used a different equation, but assumed a conceptual model of one dominant fracture set and consequently obtained a stress-versus-permeability function similar to that of DOE2. BGR used Equation (1) and, calibrated it against the Yucca Mountain data assuming three orthogonal fracture sets, similar to DOE1 and JAEA. However, BGR ended up with a function somewhat more stress sensitive. The main reason for the apparent stress-sensitivity of the function used by BGR is that they assumed an initial permeability of 1×10^{-13} m^2 rather than 3.3×10^{-13} m^2 (see Figure 7a permeability values at the initial repository stress range). A smaller initial permeability leads to a smaller initial aperture and to a smaller

residual aperture and corresponding smaller residual permeability in the BGR stress-versus-permeability function.

In the case of Type B settings, no site-specific field measurements of the thermal-mechanically-induced permeability change exist; thus, the research teams had to resort to observations from similar crystalline rock sites or laboratory data. DOE and BGR derived their stress-versus-permeability functions from the Barton-Bandis joint model (e.g., Barton and Bakhtar 1982). These functions were developed from the Barton-Bandis aperture-versus-stress function; then, the rock-mass permeability function was derived from the cubic law and a model of regular spaced fractures. The Barton-Bandis aperture-versus-stress function may be combined with a residual aperture, b_r, and written as (Rutqvist et al. 2000):

$$b = b_r + b_m = b_r + \frac{k_{n0} V_{m0}^2}{\sigma_n + k_{n0} V_{m0}} \tag{2}$$

where k_{n0} and V_{m0} are normal stiffness and maximum closure at the zero stress intercept of the Bandis hyperbola. According to Barton and Bakhtar (1982), the basic parameters k_{n0} and V_{m0} for Equation (2) could be derived using basic Barton-Bandis joint parameters that were given for the Task B repository setting as Joint Roughness Coefficient (JRC) = 8.83, Joint Compressive Strength (JCS) = 105 MPa, and a residual friction angle of 30.3 degrees (Birkholzer et al. 2008).

The Barton-Bandis joint model also provides an empirical relationship between equivalent hydraulic and mechanical (or physical) apertures, which may be written as:

$$b_h = b^2 / JRC^{2.5} \tag{3}$$

where b_h and b are respectively equivalent hydraulic and mechanical aperture (in microns).

For the Type B setting, the resulting stress-versus-permeability functions derived by each team were also different, depending on assumptions made during the calibration. For example, Figure 7b shows that there is a significant difference in the derived stress-versus-permeability functions for DOE and BGR, which were both derived using the Barton-Bandis stress-versus-aperture function in Equation (2). The difference was a result of difference in the derivation of the effective permeability for a fractured rock and the lack of well constrained site specific data for calibrating the stress-versus-permeability functions (Birholzer et al. 2008). CAS derived a stress-versus-permeability function for the Type B repository site using the cubic relationship between fracture flow rate and fracture aperture and in which the fracture aperture is inversely proportional to fracture normal stress. When comparing the resulting stress-versus-permeability functions to literature data on both core samples and in situ experiments (Rutqvist and Stephansson, 2003), one might say that the functions generated by CAS and BGR represent two extremes of stress-versus-permeability functions in granitic rock.

5.2 Simulated Evolution of Vertical Permeability

The stress-versus-permeability functions derived by each team (as shown in Fig. 7) were then applied to estimating the evolution of permeability for both Types A and B. An example of the calculated vertical-permeability evolution is shown in Fig. 8. For both repository types, the vertical permeability decreases as a result of the closure (reduced aperture) of vertical fractures caused by the increased horizontal stress.

Figure 9 compares permeability changes calculated by each team, expressed as a permeability-change-factor defined as k/k_i, where k is the current permeability (in this case at t = 1,000 years) and k_i is the

initial (pre-excavation) permeability. The simulated permeability changes in Types A and B by the different research teams were consistent with each other in that more substantial changes occurred in the case of Type A. Specifically, for Type A, the estimated permeability decrease in the rock mass during the thermal stress peak was about one to two orders of magnitude, with the strongest decreases calculated by the BGR. For Type B, the strongest permeability decrease was a reduction of permeability to a factor of about 0.5 of its initial value, calculated by CAS. The more substantial permeability changes in the case of Type A can be understood from Figs. 6 and 7. In the Type A case, the initial stress is about 3 MPa. During heating of the rock mass, the thermal stress increases to about 15 MPa (Fig. 6a). According to Fig. 7a, such a stress increase may cause a permeability reduction by as much as one to two orders of magnitude, depending on the assumed stress-versus-permeability model. In the Type B case, the initial effective stress across the dominant vertical fracture set is as high as 27 MPa. During heating of the rock mass, the stress increases to about 45 MPa (Fig. 6b). However, according to Fig. 7b, an increase of stress from 27 to 45 MPa will cause only a minor reduction in permeability.

In Fig. 9, also note that the largest permeability reduction tends to occur near or above the drift rather than below the drift. This observation can be understood from the DOE1 results in Fig,. 8a. It shows that the initial permeability is higher as a result of a lower initial stress in the shallower parts. During heating, fractures close to a residual aperture both above and below the repository. However, the lower stress and corresponding large initial permeability causes a more substantial permeability reduction in the shallower parts.

6 Impact on the Flow Field

The results for all the research teams showed that for the repository settings considered in this study, the calculated changes in permeability had only minor impact on the regional vertical flow field, whereas the changes close to the drifts were more significant.

For Repository Type A, the vertical flow rate in the unsaturated fractured rock system is controlled by the assumed infiltration rate of 6 mm/year at the top of the model. This vertical flow rate prevails regardless of changes in the intrinsic permeability of the system. In this case, the stress-induced decrease in the vertical intrinsic fracture permeability is offset by an increase in fracture saturation and relative permeability for liquid flow. In other words, the unsaturated system corrects itself to accommodate the 6 mm/year infiltration rate.

The simulation results showed that in the case of Type A, the main impact of stress induced permeability changes may be on the dryout zone near the emplacement drift. For example, DOE found that when stress-induced changes in hydrological properties are considered, the extent of the dryout zone is slightly smaller (Fig. 10a). It was also concluded that to determine the impact of mechanically-induced changes in hydrologic properties in the near field of Type A, it is important to simulate multiphase flow processes with gas flow and liquid flow in fractures and matrix separately (Birkholzer et al. 2008). For example, JAEA used a single phase flow model and obtained the opposite results of DOE, i.e. the dryout zone would be slightly larger when considering stress-induced changes in hydrological properties. Thus, while the simplified single phase flow models applied by some of the research teams are sufficient for calculating evolution of thermal stress and permeability, they are not appropriate for investigating the impact of such permeability changes on the multiphase fluid flow behavior in the near field for a high (above boiling) temperature repository.

In the case of Repository Type B, the regional vertical permeability (i.e the vertical permeability in the rock mass outside the zone influence by stress changes around the drift) was reduced to a factor of about 0.5 of its original value when assuming the most sensitive stress-versus-permeability relationship (CAS model in Fig. 7b). As a result, the vertical flow rate could be reduced to as low as 50% of the original flow rate. The excavation of the drift resulted in local permeability increases of up to two orders of magnitude near the drift wall, resulting in an increased flow rate around the drift. However, an increased permeability around the drift would be more relevant when considering flow along the tunnel rather than vertical flow across the tunnel.

7 Concluding Remarks

In this study, we conducted a comparative simulation study of coupled thermal, hydrological, and mechanical (THM) interactions and their impact on permeability and fluid flow around heated underground nuclear waste emplacement drifts in fractured rock. Simulations were conducted considering two types of repository settings: (a) open emplacement drifts in relatively shallow, unsaturated volcanic rocks, and (b) backfilled emplacement drifts in deeper, saturated crystalline rocks. In general, predicting mechanically induced changes in fracture rock permeability is a difficult task, given the great uncertainties related to predicting complex mechanical and hydromechanical processes in fractured rock. However, with an accurate calculation of stress evolution, resulting changes in hydrological properties of the fractured rock mass may be bounded by conservative choices of relationships between permeability and stress within a fractured rock mass.

This analysis shows that the main stress response in both repository settings is an increase in horizontal thermal stress that has two possible consequences on the permeability field. First, an increased horizontal stress tends to reduce the aperture and permeability in steeply dipping fractures. Second, an increased horizontal stress also leads to increased shear stress that could induce shear failure and dilation of shallowly dipping fractures. For the assumed properties and repository settings in this study, shear-induced permeability changes were ruled out, because the shear stresses were not sufficiently high or because shallowly dipping fractures were considered minor—judged not to significantly contribute to fluid flow. This led to a system in which permeability changes during the heating period were controlled by a reduction in vertical permeability, caused by horizontal thermal stress. This reduction in permeability critically depends on (1) an accurate prediction of regional thermal-mechanical stress evolution, and (2) a correctly bounded estimate of the relationship between stress and permeability for fractured rock.

The study showed that predicting the regional thermal-mechanical stress evolution in the rock mass can be done with a high confidence level, because this evolution is controlled by regional heat conduction and thermal-mechanical expansion, processes that are relatively insensitive to local heterogeneities such as rock fractures. Moreover, the regional thermal-mechanical stress evolution is insensitive to complex near-field multiphase flow processes. On the other hand, the stress-versus-permeability relationship of the rock mass is much more uncertain, because it critically depends on complex local mechanical and hydromechanical interactions of fractures. In this study, different research teams derived a wide range of stress-versus-permeability relationships, based on field experiments and literature data representative for the two repository settings. However, even for the most sensitive relationships between stress and permeability, the impact of mechanically induced changes in permeability on the flow field was relatively small, with most changes occurring in the vicinity of the emplacement drifts.

Although the impact of mechanically induced permeability changes was small for the hypothetical repository setting assumed in study, this conclusion cannot necessarily be generalized to other sites. The potential impact of THM processes on hydrological properties has to be done on a case-by-case basis, since the outcome depends on site specific in situ stress field and fracture characteristics. At any site, the evaluation of the potential for and significance of shear-induced permeability changes may be the most challenging and uncertain aspect of this type of analysis. Moreover, the potential coupling to chemical processes (i.e. THMC), for example by thermally enhanced pressure solution of fracture surface asperities (Min et al. 2008), may also be important for some geological and repository conditions.

Acknowledgments

Review comments by Ki-Bok Min, University of Adelaide, Australia and Dan Hawkes at the Lawrence Berkeley National Laboratory are greatly appreciated. Funding to LBNL for the work done by the LBNL authors was provided by the U.S. Department of Energy under Contract No. DE-AC02-05CH11231. The United States Government retains and the publisher, by accepting the article for publication, acknowledges that the United States Government retains a non-exclusive, paid-up, irrevocable, world-wide license to publish or reproduce the published form of this manuscript, or allow others to do so, for United States Government purposes. Funding for modeling work by other research teams was provided by Japan Atomic Energy Agency (JAEA), the Federal Institute for Geosciences and Natural Resources (BGR), and the National Nature Science Foundation of China under Grant No. 50709036, 40520130315.

It is emphasized that the views expressed in this paper are solely those of the authors and cannot necessarily be taken to represent the views of any of the organizations or individuals listed above.

References

Alonso EE et al. (2005) The FEBEX bechmark test. Case definition and comparison of modelling approaches. Int J Rock mech & Min Sci 42:611–638.

Barton N R, Bakhtar K (1982) Rock joint description and modeling for the hydrothermomechanical design of nuclear waste repositories. Technical Report 83-10, TerraTek Engineering, Salt Lake City, Utah.

Barton CA, Zoback MD, Moos D (1995) Fluid flow along potentially active faults in crystalline rock. Geology, 23:683–686.

Birkholzer J, Rutqvist J, Sonnenthal E, Barr D (2008) Long-term permeability/porosity changes in the EDZ and near field due to THM and THC Processes in volcanic and crystalline-bentonite systems. DECOVALEX-THMC Project, Task D. Final Report. Swedish Nuclear Power Inspectorate (SKI) Technical Report (in press).

Börgesson L, Chijimatsu M, Nguyen TS, Rutqvist J, Jing L (2001) Thermo-hydro-mechanical characterization of a bentonite-based buffer material by laboratory tests and numerical back analyses. Int J Rock Mech & Min Sci 38:105–127.

Chijimatsu M, Fujita T, Kobayashi A, Nakano M (2000) Experiment and validation of numerical simulation of coupled thermal, hydraulic and mechanical behaviour in the engineered buffer materials. Int J Numer Anal Meth Geomech 24:403–424.

Chijimatsu M, Nguyen TS, Jing L, de Jonge J, Kohlmeier M, Millard A, Rejeb A, Rutqvist J, Souley M, Sugita Y (2005) Numerical study of the THM effects on the near-field safety of a hypothetical nuclear waste repository – BMT1 of the DECOVALEX III project. Part 1: Conceptualization and characterization of the problems and summary of results. Int. J Rock mech & Min Sci 42:720–730.

de Jonge J, Xie M, Kolditz O (2004) Numerical implementation of thermally and hydraulically coupled processes in non-isothermal porous media. In: Stephansson O, Hudson JA, Jing L, editors. Coupled T-H-M-C Processes in Geo-Systems: Fundamentals, Modelling, Experiments and Applications. Elsevier Geo-Engineering Book Series, Oxford, 205–210.

Jaeger JC, Cook NGW (1979). Fundamentals of Rock Mechanics. London: Chapman and Hall.

Kolditz O, Bauer S, Beinhorn M, de Jonge J, Kalbacher T, McDermott C, Wang W, Xie M, Kaiser R, Kohlmeier M (2003) ROCKFLOW - Theory and Users Manual, Release 3.9, Groundwater Group, Center for Applied Geosciences, University of Tübingen, and Institute of Fluid Mechanics, University of Hannover.

Liu Q, Zhang C, Liu X (2006a) A practical method for coupled THM simulations of the Yucca Mountain and FEBEX case samples for task D of the DECOVALEX-THMC Project. Proc. GEOPROC2006 International symposium: 2nd International Conference on Coupled Thermo-hydro-mechanical-chemical processes in Geosystems and Engineering, HoHai University, Nanjing, China, May 22–25, 2006, 220–225, HoHai University.

Liu X, Zhang C, Liu Q (2006b) Analysis of uncertainty in coupled THM simulations of the FEBEX case example for Task D of the DECOVALEX-THMC project. Proc. GEOPROC2006 International symposium: 2nd International Conference on Coupled Thermo-hydro-mechanical-chemical processes in Geosystems and Engineering, HoHai University, Nanjing, China, May 22–25, 2006, 234–239, HoHai University.

Millard A, Rejeb A, Chijimatsu M, Jing L, de Jonge J, Kohlmeier M, Nguyen TS, Rutqvist J, Souley M, Sugita Y (2005) Numerical study of the THM effects on the near-field safety of a hypothetical nuclear waste repository – BMT1 of the DECOVALEX III project. Part 2: Effects of THM coupling in continuous and homogeneous rock. Int J Rock Mech & Min Sci 42:731–744.

Min KB, Rutqvist J, Elsworth D (2008) Chemically- and mechanically-mediated influences on the transport and mechanical characteristics of rock fractures. Int J Rock Mech & Min Sci (In press, doi.org/10.1016/j.ijrmms.2008.04.002).

Nguyen TS, Börgesson L, Chijimatsu M, Rutqvist J, Fujita T, Hernelin J, Kobayashi A, Onishi Y, Tanaka M, Jing L (2001) Hydro-mechanical response of a fractured rock mass to excavation of a test pit – The Kamaishi Mine Experiment in Japan. Int J Rock Mech & Min Sci 38:79–94.

Noorishad J, Tsang C-F (1996) Coupled thermohydroelasticity phenomena in variable saturated fractured porous rocks—Formulation and numerical solution. In O. Stephansson, L. Jing,, and C.-F. Tsang, editors, Coupled Thermo-hydro-mechanical Processes of Fractured Media. Developments in Geotechnical Engineering, Elsevier, 79:93–134.

Ohnishi Y, Shibata H, Kobayashi A (1987) Development of finite element code for the analysis of coupled thermo-hydro-mechanical behavior of a saturated-unsaturated medium. In C.-F. Tsang, editor, Coupled Processes Associated with Nuclear Waste Repositories, Academic Press, 551–557.

Ohnishi Y, Kobayashi A (1996) THAMES. In O. Stephansson, L. Jing, and C.-F. Tsang, editors, Coupled Thermo-hydro-mechanical Processes of Fractured Media, Developments in Geotechnical Engineering, Elsevier, 79:545–549.

Rutqvist J, Stephansson O (2003) The role of hydromechanical coupling in fractured rock engineering. Hydrogeology Journal 11:7–40.

Rutqvist J, Tsang C-F (2003) Analysis of thermal-hydrologic-mechanical behavior near an emplacement drift at Yucca Mountain. Journal of Contaminant Hydrology 62–63:637–652.

Rutqvist J, Stephansson O, Tsang C-F (2000) Uncertainty in estimate of maximum principal stress from hydraulic fracturing due to the presence of the induced fracture. Int J Rock Mech & Min Sci 37;107–120.

Rutqvist J, Börgesson L, Chijimatsu M, Kobayashi A, Nguyen TS, Jing L, Noorishad J,Tsang C-F (2001a) Thermohydromechanics of partially saturated geological media – Governing equations and formulation of four finite element models. Int J Rock Mech Min Sci 38:105-127.

Rutqvist J, Börgesson L, Chijimatsu M, Nguyen TS, Jing L, Noorishad J, Tsang CF (2001b) Coupled thermo-hydro-mechanical analysis of a heater test in fractured rock and bentonite at Kamaishi Mine – Comparison of field results to predictions of four finite element codes. Int J Rock Mech & Min Sci 38:129–142.

Rutqvist J, Wu YS, Tsang C-F, Bodvarsson G (2002) A modeling approach for analysis of coupled multiphase fluid flow, heat transfer, and deformation in fractured porous rock. Int J Rock mech & Min Sci 39:429–442.

Rutqvist J, Barr D, Datta R, Gens A, Millard M, Olivella S, Tsang C-F, Tsang Y (2005a) Coupled thermal-hydrological-mechanical analysis of the Yucca Mountain Drift Scale Test – comparison of field results to predictions of four different models. Int J Rock Mech & Min Sci 42:680–697.

Rutqvist J, Chijimatsu M, Jing L, de Jonge J, Kohlmeier M, Millard A, Nguyen TS, Rejeb A, Souley M, Sugita Y, Tsang C-F. (2005b) Numerical study of the THM effects on the near-field safety of a hypothetical nuclear waste repository – BMT1 of the DECOVALEX III project. Part 3: Effects of THM coupling in fractured rock. Int J Rock Mech & Min Sci 42:745–755.

Rutqvist J, Barr D, Birkholzer JT, Chijimatsu M, Kolditz O, Liu Quansheng, Oda Y, Wang Wengqing, Zhang Chenyuan (2008a) Results from an international simulation study on coupled thermal, hydrological, and mechanical (THM) processes near geological nuclear waste repositories. Nuclear Technology 163:101–109.

Rutqvist J, Freifeld B, Min K-B, Elsworth D, Tsang Y (2008b) Analysis of thermally induced changes in fractured rock permeability during eight years of heating and cooling at the Yucca Mountain Drift Scale Test. Int J Rock Mech & Min Sci (In press, doi.org/10.1016/j.ijrmms.2008.01.016).

Tsang YW, Birkholzer JT (1999) Predictions and observations of the thermal-hydrological conditions in the single heater test. Journal of Contaminant Hydrology 38:385–425.

Tsang CF et al. (2008) Advances in Modeling Coupled Thermo-Hydro-Mechanical-Chemical Processes in Geological Formations: an Overview of the DECOVALEX-THMC Project. Environmental Geology (this issue).

Wang J, Cook P (2005) Air-permeability distributions at niches in tuff units at Yucca Mountain. Proceedings of the 40th U.S. Rock Mechanics Symposium, Anchorage, Alaska, USA, 25-29 June, 2005: American Rock Mechanics Association ARMA, Paper No. 846.

Wang W, Xie M, Nowak T, Kunz H, Shao H, Kolditz O (2006) Modeling THM coupled problem of Task D of the DECOVALEX project. Proc. GEOPROC2006 International symposium: 2nd International Conference on Coupled Thermo-hydro-mechanical-chemical processes in Geosystems and Engineering, HoHai University, Nanjing, China, May 22-25, 2006, 226–232, HoHai University.

Xie M, Wang W, Nowak T, Kunz H, Shao H, Kolditz O (2006) Numerical simulation of a THC problem and its long-term effect on bentonite/granite FEBEX type repository. Proc. GEOPROC2006 International symposium: 2nd International Conference on Coupled Thermo-hydro-mechanical-chemical processes in Geosystems and Engineering, HoHai University, Nanjing, China, May 22-25, 2006, 403–410, HoHai University.

Zimmerman RM, Wilson ML, Board MP, Hall ME, Schuch RL (1985) Thermal-cycle testing of the G-tunnel heated block. Proceedings of the 26th US Symposium on Rock Mechanics, Rapid City, SD, 26-28 June 1985, AA Balkema, Rotterdam 749–758.

Zimmerman RM, Schuch RL, Mason RL, Wilson ML, Hall ME, Board MP, Bellman RP, Blandford ML (1986) Final report: G-Tunnel Heated Block Experiment. SAND84-2620, Sandia National Laboratory, Albuquerque, NM.

Table 1. Research teams and numerical simulators applied in this study.

Research Team	Numerical Simulator	Brief Description of Numerical Simulator
DOE U.S. Department of Energy's Research Team: Lawrence Berkeley National Laboratory (LBNL)	TOUGH-FLAC	TOUGH-FLAC is a simulator for analysis of coupled THM processes under multiphase fluid flow conditions being developed at the LBNL (Rutqvist et al, 2002). The simulator is based on linking of the existing computer codes TOUGH2 and FLAC3D. It has been extensively used for analysis of coupled THM processes within the Yucca Mountain Project (e.g. Rutqvist and Tsang 2003).
	ROCMAS	ROCMAS is a finite element program for analysis of coupled THM processes in porous and fractured rock developed at LBNL (Noorishad and Tsang 1996, Rutqvist et al. 2001a). In the late 1990s, this code was extended to unsaturated media with single-phase liquid flow and vapor diffusion in a static gas phase The code has been extensively applied in earlier phases of the DECOVALEX project for THM analysis in bentonite-rock systems (Nguyen et al. 2001, Rutqvist et al. 2001b, Rutqvist et al. 2005b).
BGR Bundesanstalt für Geowissenschaften und Rohstoffe's Research Team: University of Tübingen	GeoSys/ Rockflow	GeoSys/Rockflow is based on object-oriented programming and is developed at the University of Tübingen (Kolditz et al. 2003). It was first applied in previous DECOVALEX phases for analysis of thermal-hydrological and thermal-mechanical processes and has been extended to THM (de Jonge et al. 2004; Wang et al. 2006) and reactive chemical transport analysis (Xie et al. 2006). For the present study, an unsaturated single-phase liquid flow and vapor diffusion is considered.
CAS Chinese Academy of Sciences' Research Team	FRT-THM	The FRT-THM (Fluid-Rock Transport simulator) being developed by the CAS is based on MATLAB and C language codes, in which FEMLAB is used as partial differential equation solver (Liu et al. 2006). The approach being developed for the present study features an unsaturated single-phase fluid flow and vapor diffusion model approach (Liu et al. 2006a; Liu et al. 2006b)
JAEA Japan Atomic Energy Agency's Research Team, including Hazama Cooperation	THAMES	THAMES is a finite element program for analyzing coupled THM processes in porous and fractured rock developed at the Kyoto University (Ohnishi et al. 1987; Ohnishi and Kobayashi, 1996). The code has been extended to unsaturated media with single-phase liquid flow and vapor diffusion in a static gas phase (Chijimatsu et al. 2000). The THAMES code has been extensively applied in earlier phases of the DECOVALEX project for THM analysis in bentonite-rock systems (e.g. Börgesson et al. 2001; Chijimatsu et al. 2005; Millard et al. 2005).

Table 2. Model dimensions and thermal line loads (See Fig. 1)

Repository design	Type A: High temperature, open drift	Type B: Low temperature, backfilled drift
Model height, Lz1 (m)	250	500
Model height, Lz2 (m)	350	500
Drift spacing, Lx (m)	51	35
Drift diameter, ϕ (m)	5.5	2.28
Max. thermal line load, Pw (w/m)	592 (at 50 years)*	245 (at emplacement)

*Heat load is assumed to be reduced by drift ventilation until 50 years

Table 3. Some basic THM rock properties

Parameter	Type A: Volcanic Tuff*	Type B: Granite
Bulk Density, [kg/m^3]	2370	2700
Matrix Porosity [-]	0.13	0.01
Young's Modulus, [GPa]	15	35
Poisson's ratio, [-]	0.21	0.3
Specific heat, [J/kg·°C]	985	900
Thermal conductivity, [W/m·°C]	2.29	3.0
Thermal expansion coefficient, [°C^{-1}]	1.0×10^{-5}	1.0×10^{-5}
Bulk Permeability, [m^2]	3.3×10^{-13}	1.0×10^{-17}

*The complete data set for welded tuff includes multiphase (e.g., retention and relative permeability data for gas and liquid) fluid flow properties for matrix and fracture continua.

Table 4. Initial conditions

Parameter	Type A: Volcanic unsaturated rock	Type B: Crystalline saturated rock
Repository depth (m)	250	500
Temperature (ºC)	T = 18+0.028×D	T = 10+0.030×D
Water Pressure	Unsaturated system with ground water table at 550 m depth	Hydrostatic with ground water table at the ground surface
Vertical stress (MPa)	$\sigma_v = 0.0232\times D$	$\sigma_v = 0.0265\cdot\times D$
Maximum horizontal stress (MPa)	$\sigma_h = 0.0138\times D$	$\sigma_H = 4.6+0.055\cdot\times D$
Minimum horizontal stress (MPa)	$\sigma_h = 0.0115\times D$	$\sigma_h = 0.6+ 0.020\times D$

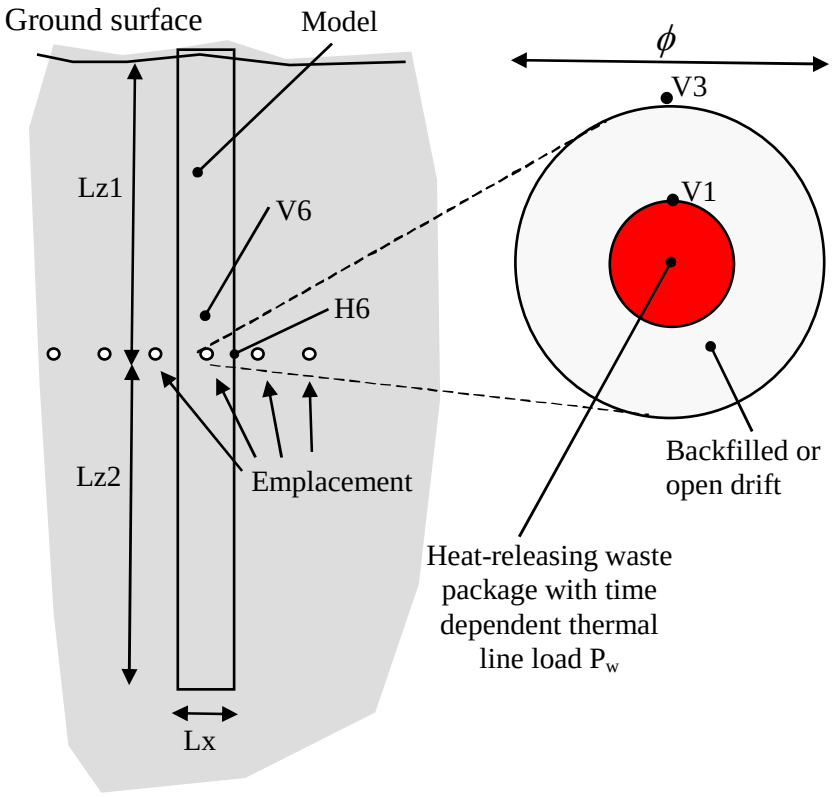

Figure 1. Model geometry for Repository Types A and B (see Table 2 for dimensions and heat load).

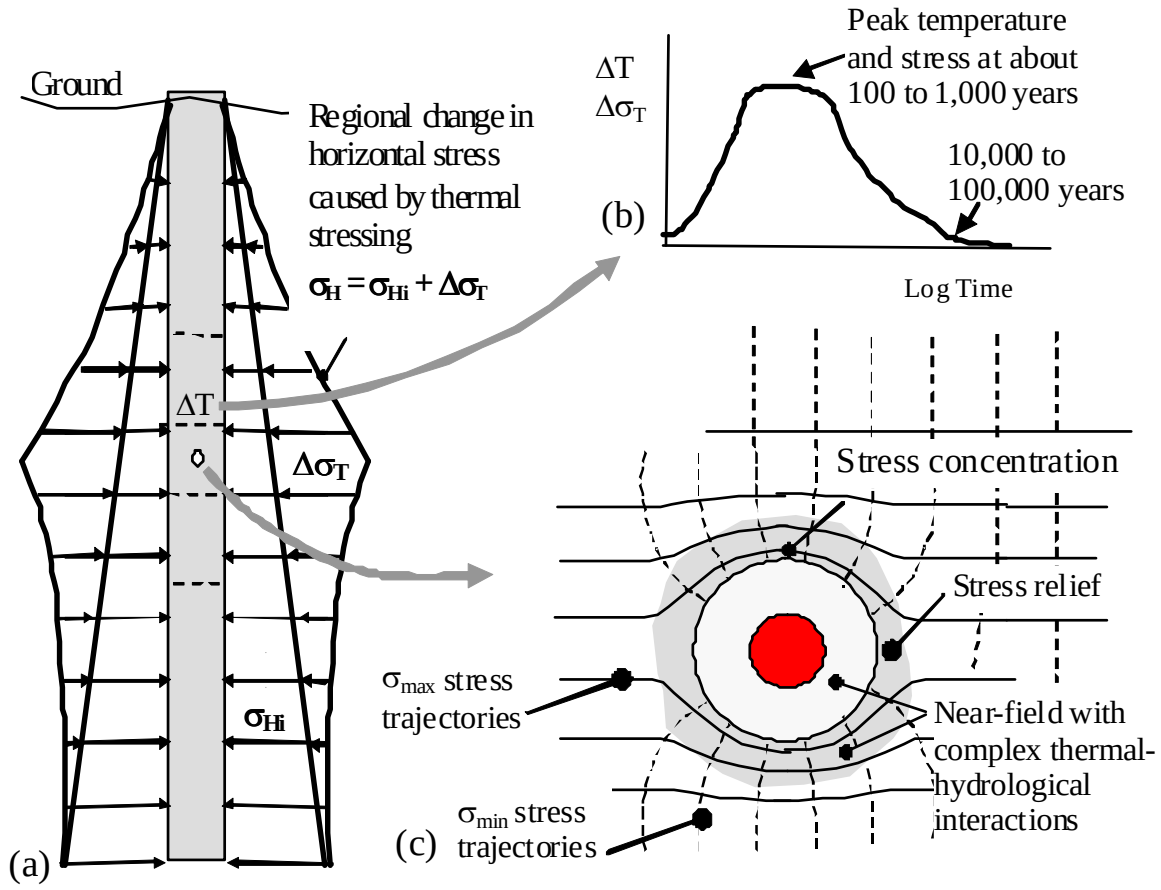

Figure 2. Schematic of main thermal-mechanical responses common for both Repository Types A and B.

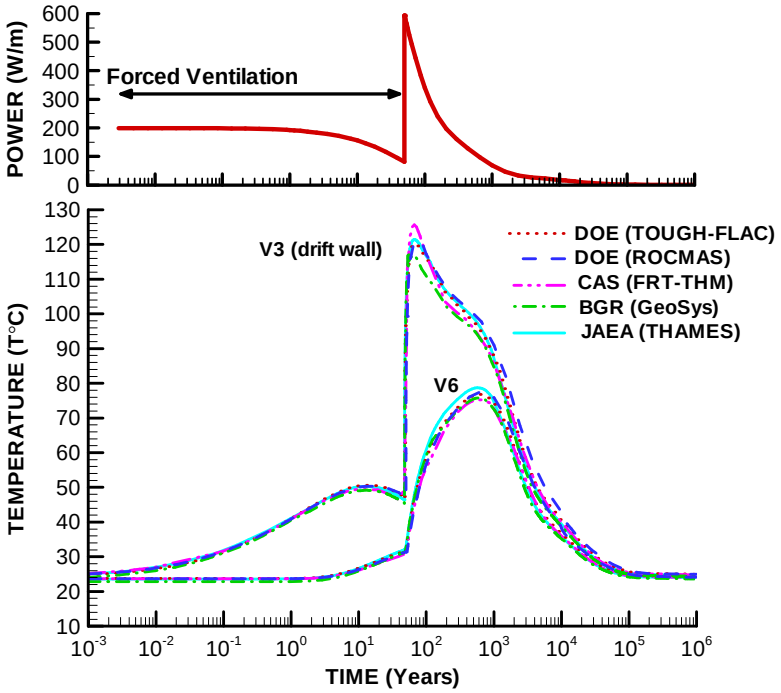

(a)

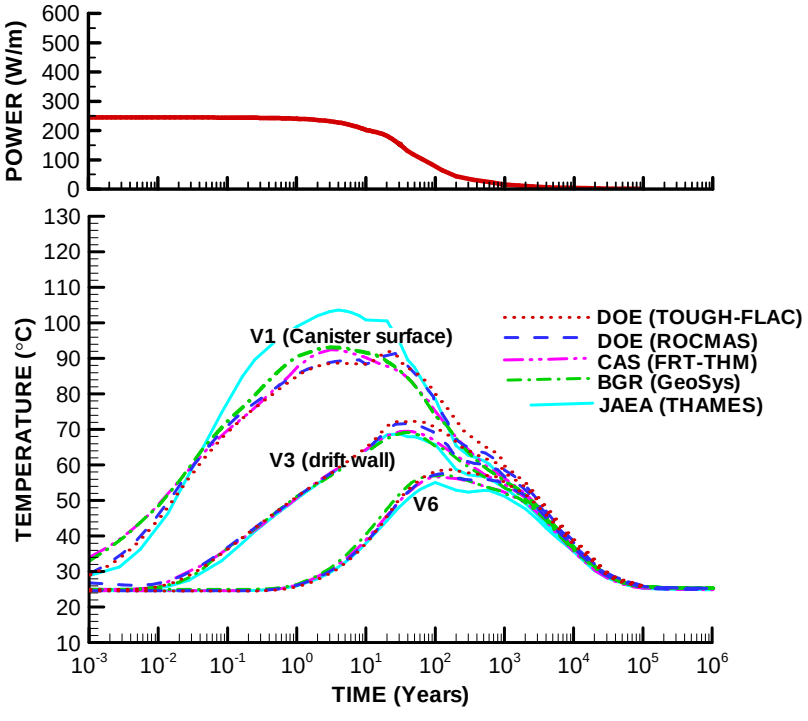

(b)

Figure 3. Evolution of calculated power and temperature for (a) Repository Type A and (b) Repository Type B. Locations of points V1, V3 and V6 are indicated in Fig. 1.

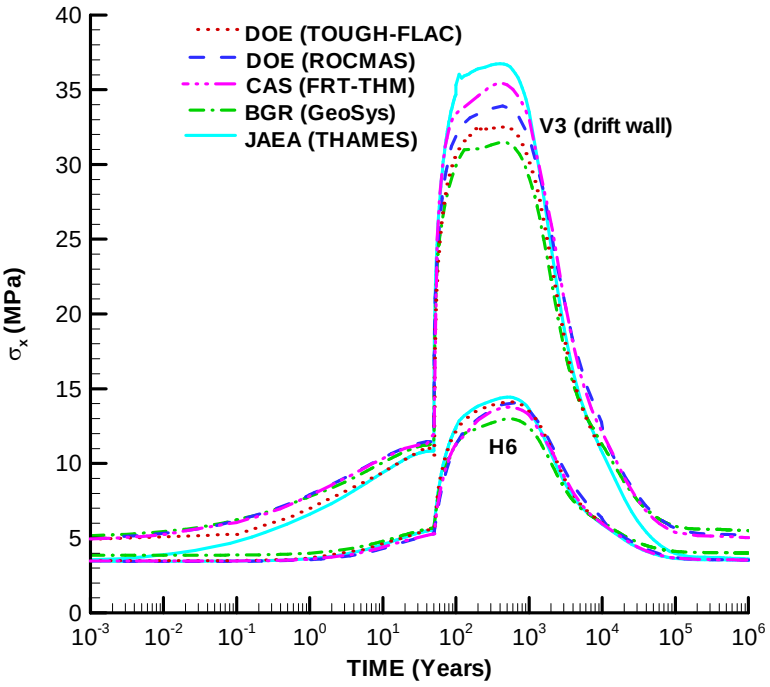

(a)

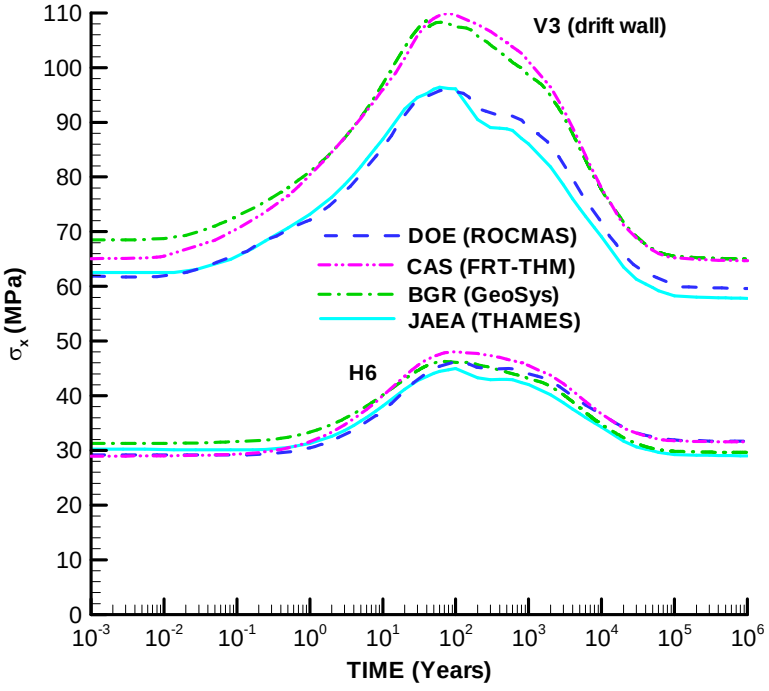

(b)

Figure 4. Evolution of calculated horizontal stress for (a) Repository Type A and (b) Repository Type B. Locations of points V3 and H6 are indicated in Fig. 1.

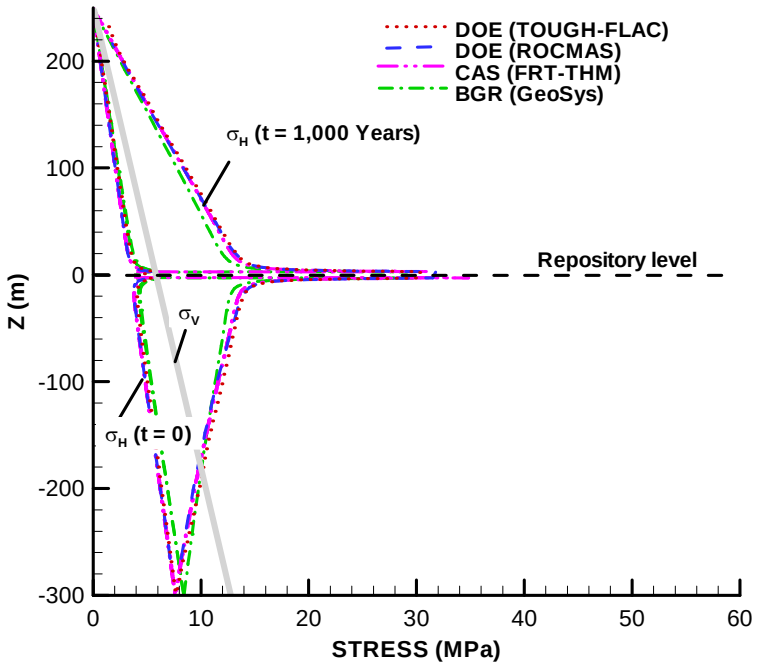

(a)

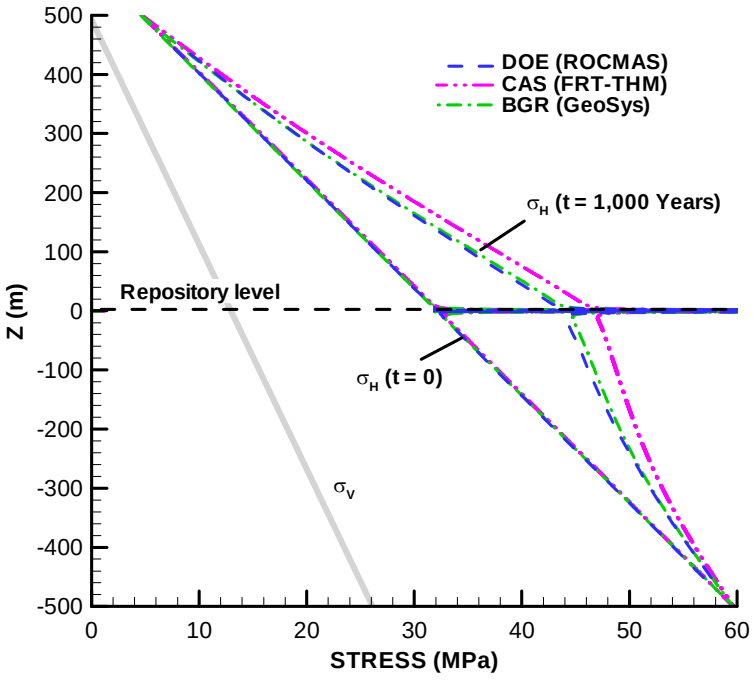

(b)

Figure 5. Comparison of profiles of stress for (a) Repository Type A and (b) Repository Type B.

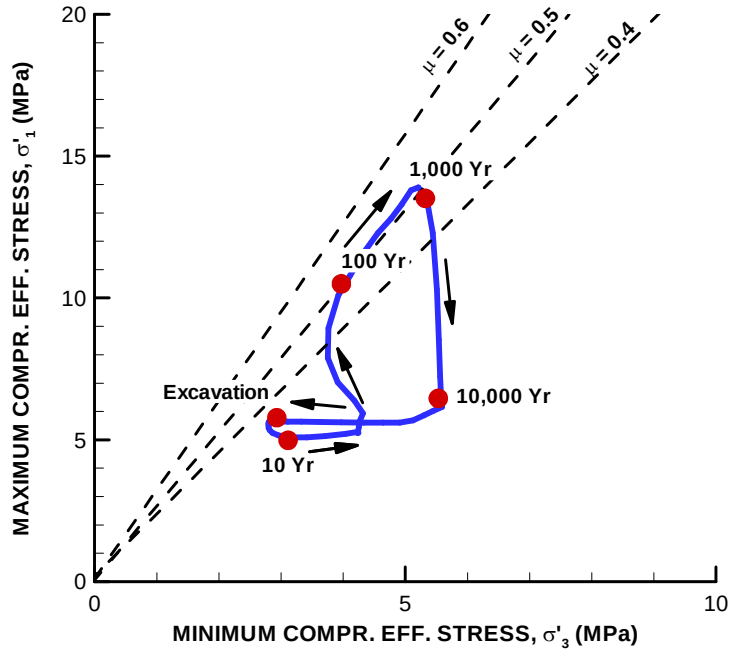

(a)

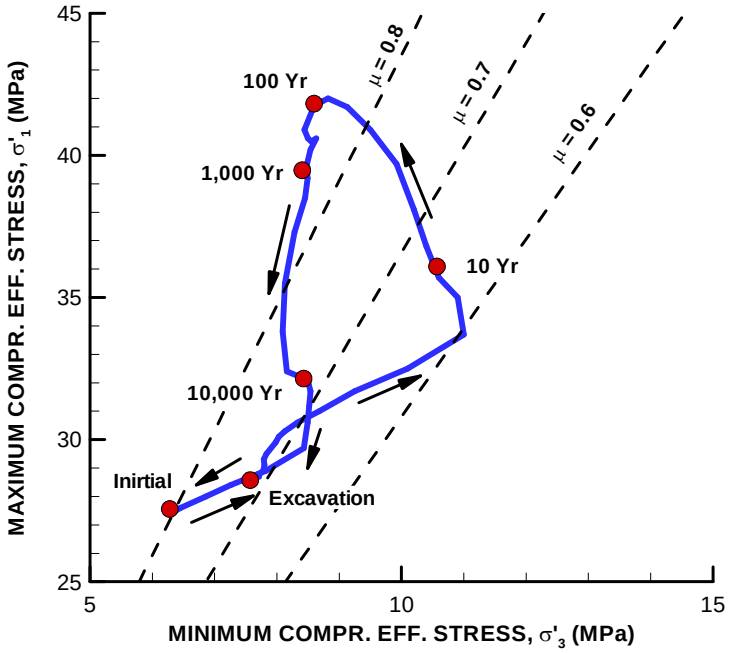

(b)

Figure 6. Evolution of the principal stress ratio in relation to stress ratios that could be sustained for different values of the coefficient friction (μ) of arbitrarily oriented pre-existing fractures for (a) Repository Type A and (b) Repository Type B (DOE analysis).

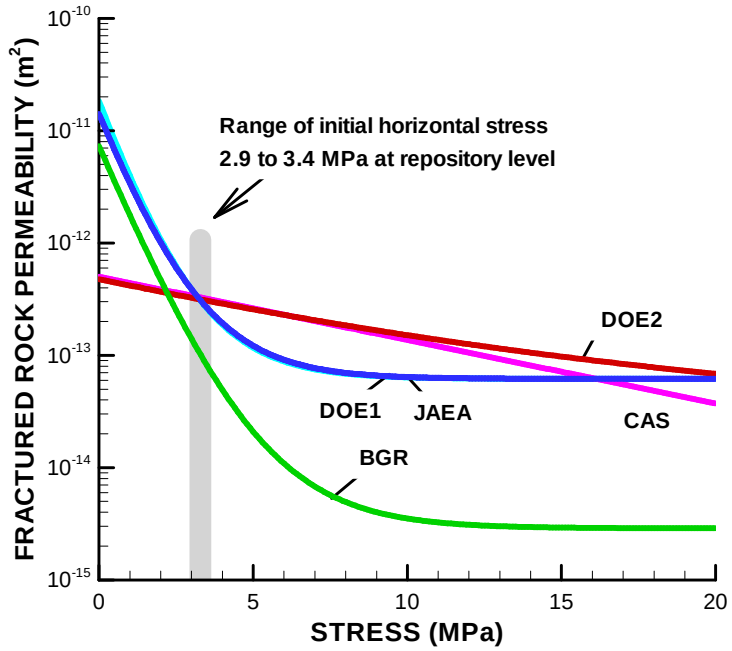

(a)

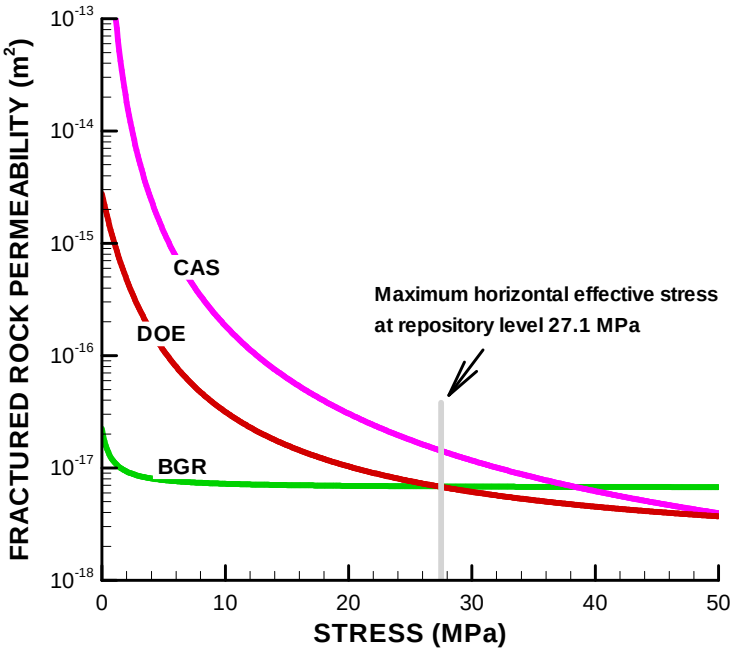

(b)

Figure 7. Comparison of resulting stress-versus-permeability relationships for fractured rock permeability: (a) Repository Type A; (b) Repository Type B

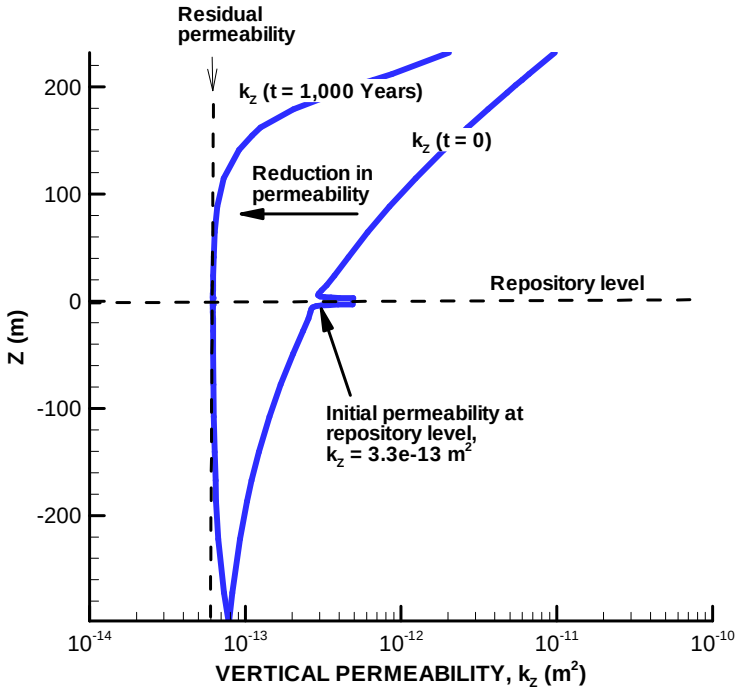

(a)

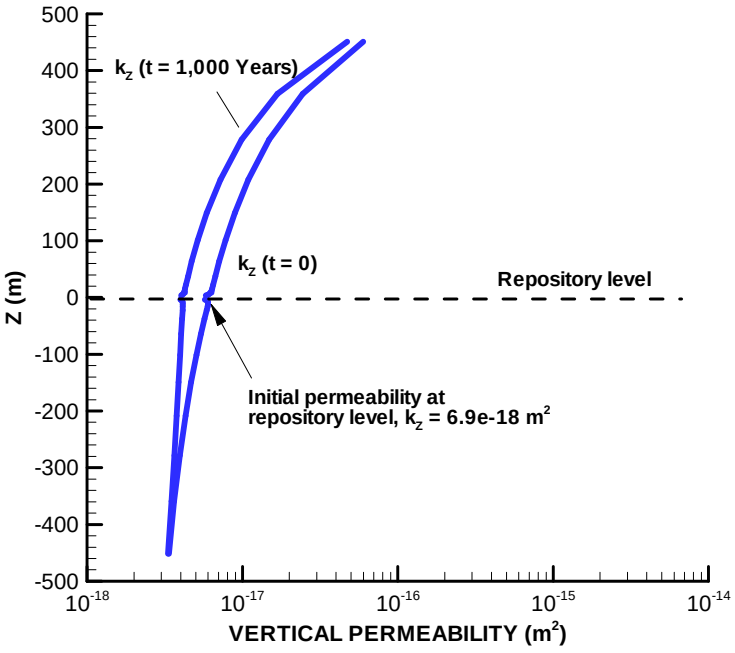

(b)

Figure 8. Calculated vertical permeability at t = 0 and 1,000 years using the DOE1 stress-versus-permeability function for (a) Repository Type A and (b) Repository Type B.

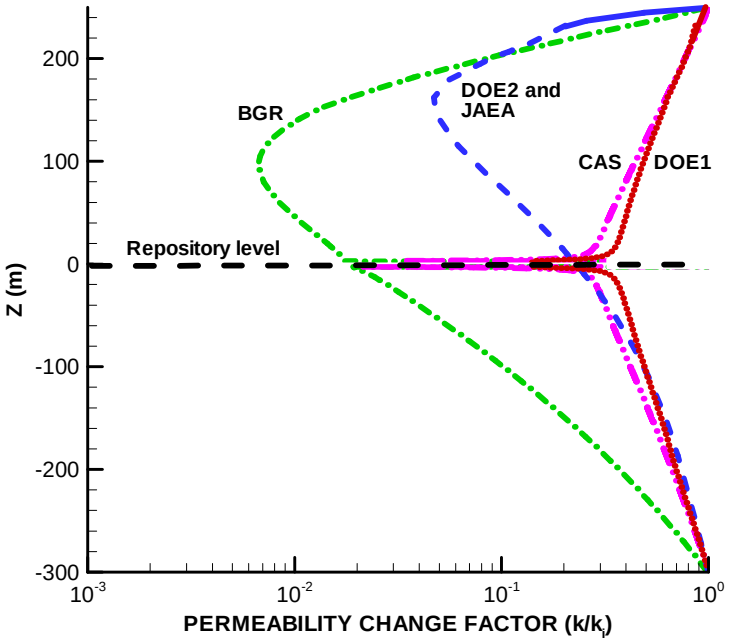

(a)

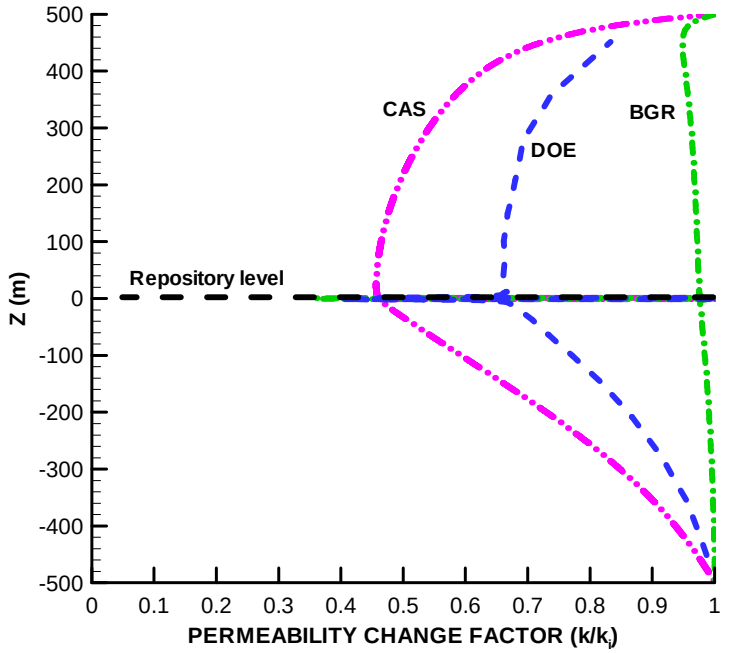

(b)

Figure 9. Comparison of calculated changes in vertical permeability at t = 1,000 years for (a) Repository Type A and (b) Repository Type B. Note that the permeability axis ranges over three orders of magnitude in (a), whereas it ranges over only one order of magnitude in (b),

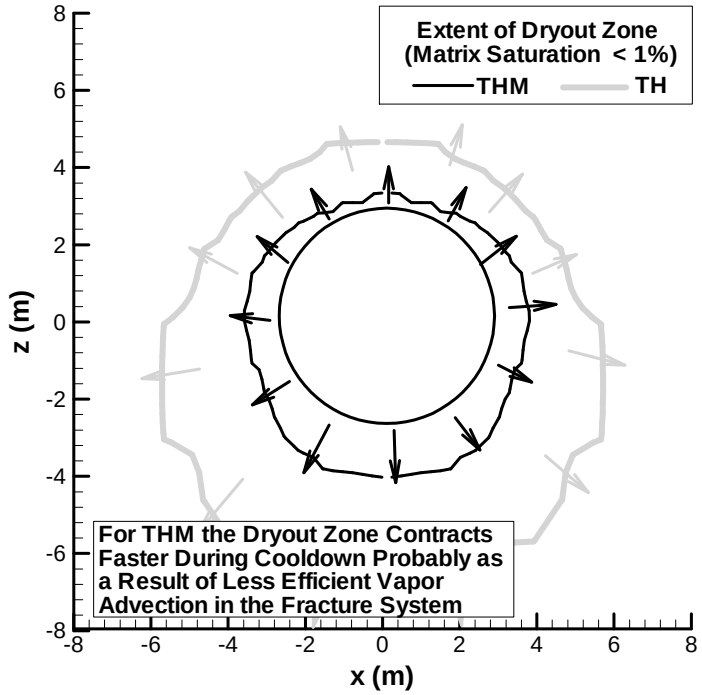

(a)

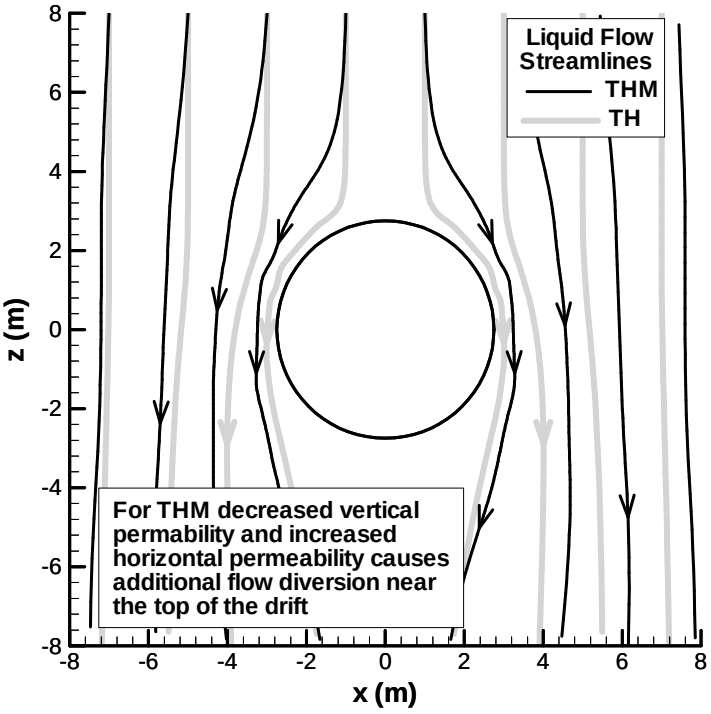

(b)

Figure 10. Near-field impact of mechanically induced changes in hydrological properties for Repository Type A: (a) impact on the extent of the dryout zone after 1,000 years, and (b) impact on the liquid-fluid-flow pattern at 10,000 years (DOE1 analysis). Mechanically induced changes in permeability are considered in the THM results, but not in the TH results.